ADVANCED FUNCTIONAL MATERIALS
www.afm-journal.de

A Li/Mg Double-Salt Strategy Based on Amine Solvent Achieves Bulk Phase-Interface-Electrode Multi-Scale Optimization for Mg Metal Batteries

Fei Wang, Haiming Hua, Yichao Zhuang, Jiayue Wu, Jing Zeng, and Jinbao Zhao**

Achieving good compatibility between anodes and cathodes with electrolytes still faces great challenges in Mg metal batteries (MMBs). Recently developed amine-based electrolytes have enabled reversible Mg anodes with conventional Mg salts through solvation structure regulations but still suffer from low conductivity and poor cathode compatibility. Herein, a Li/Mg double-salt strategy is proposed to achieve the bulk phase-interface-electrode multi-scale optimization for the amine-based electrolyte, including ionic conductivity, anode stability, and cathode compatibility. Lithium triflate (LiOTf) serves as a multifunctional additive to compensate for the limitations of single Mg salt electrolyte ($MgCl_2$/3-methoxypropylamine). Li^+ ions accelerate the ions transport in the bulk phase and ions insertion at the cathode side, benefitting to the conductivity and the cathode compatibility. Attributed to the high reduction stability of OTf^- anions, the stable Mg anode/interface is also retained. Therefore, the Mg//SS cell achieves an ultralong cycling life for 2100 cycles with the coulombic efficiency of 99.8% at 1.0 mA cm^{-2} and the full cell also exhibits a superior cycling performance for 1000 cycles at 5 C. Additionally, the batteries with the optimized electrolyte are verified as a proof-of-concept for the air-assembled MMBs. This work emphasizes the crucial role of multifunctional additives in enhancing amine-based electrolyte performances.

1. Introduction

Magnesium (Mg) metal is an attractive alkaline earth metal with divalent properties, high natural abundance, and relatively uniform electrodeposition morphology. Therefore, it exhibits great potential as a novel metal anode attributed to corresponding high volumetric energy density, low price, and good safety.[1] Benefitting from these, Mg metal batteries (MMBs) have attracted much attention as a new electrochemical energy-storage system.[2] The superiority of MMBs is mainly based on the efficient utilization of Mg metal anode. Consequently, the most crucial requirement of MMBs is the highly reversible deposition/stripping behavior for Mg metal anode. However, this basic requirement for Mg anode cannot be met as expected. Because of the divalent Mg^{2+} ion with an intrinsic property of high charge density and strong electrostatic interaction, the large desolvation energy barrier and sluggish diffusion kinetic in the Mg metal anode/electrolyte interface will lead to severe anode passivation effect, showing the ultrahigh polarization and the extremely low coulombic efficiency (CE).[3] The failure of Mg metal anode brings great challenges to MMBs and hinders the application of MMBs seriously.

Rational electrolyte design is an effective approach to optimize the compatibility between electrolyte and Mg metal anode. For example, reductive electrolytes including Grignard-based[4] and boron-based electrolytes[5] avoid the formation of passivation layers in thermodynamics and thus achieve reversible Mg anode. However, these electrolytes still suffer from formidable challenges such as high prices of raw materials, complicated synthesis methods, and especially, deliberate electrolyte preparation processes due to the high sensitivity to water and oxygen. These intractable factors impede their potential for commercialization at present. In comparison, the traditional electrolytes (commercially available Mg salts and solvents) which were previously considered to be prone to passivate the Mg anode have successfully achieved reversible Mg deposition/stripping behaviors in recent years through the introduction of strong coordination ability solvents to achieve solvation sheath reorganization (such as amine-type solvents), and show great potentials for commercialization.[6] The solvation structure regulation accelerates the interfacial charge transfer kinetics and lowers the desolvation energy barrier, thereby avoiding the unfavorable decomposition of electrolyte components in kinetics. Besides, the strong hydrogen bonding ability of the amino-group can restrain the activity of water molecules to reduce the adverse influences of impurity water in the electrolytes on the anode

F. Wang, H. Hua, Y. Zhuang, J. Wu, J. Zeng, J. Zhao
College of Chemistry and Chemical Engineering
State-Province Joint Engineering Laboratory of Power Source Technology for New Energy Vehicle
State Key Laboratory of Physical Chemistry of Solid Surfaces
Engineering Research Center of Electrochemical Technology
Ministry of Education
Collaborative Innovation Center of Chemistry for Energy Materials
Xiamen University
Xiamen 361005, P. R. China
E-mail: zengjing@xmu.edu.cn; jbzhao@xmu.edu.cn

The ORCID identification number(s) for the author(s) of this article can be found under https://doi.org/10.1002/adfm.202414181

DOI: 10.1002/adfm.202414181

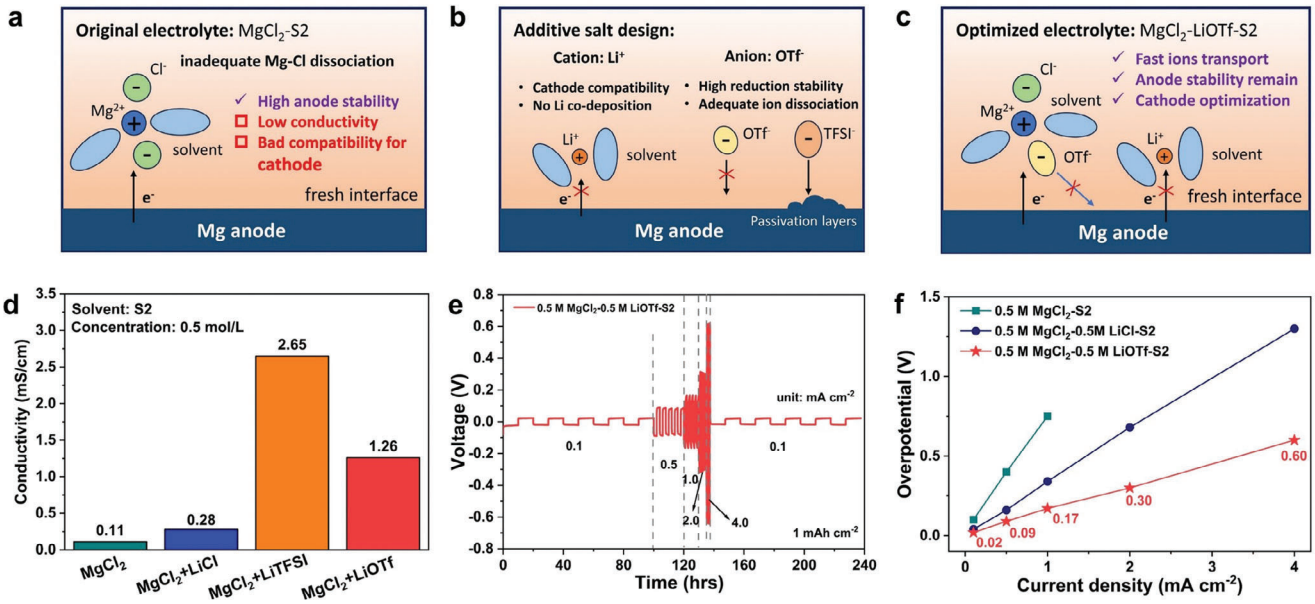

Figure 1. a) Schematic illustration of solvated structures and characteristics of the original $MgCl_2$-S2 electrolyte. b) Schematic illustration of the additive design idea for cation and anion. c) Schematic illustration of solvated structures and characteristics of the optimized $MgCl_2$-LiOTf-S2 electrolyte. d) The conductivities of the original electrolytes with different additive salts. e) Rate performance of the $MgCl_2$-LiOTf-S_2 electrolyte at various current densities from 0.1 to 4.0 mA cm^{-2} (0.1, 0.5, 1.0, 2.0, 4.0, and 0.1 mA cm^{-2} with 1.0 mAh cm^{-2}) in the symmetrical Mg//Mg coin cell. f) Comparison of the overpotentials of $MgCl_2$-S2, $MgCl_2$-LiCl-S2 and $MgCl_2$-LiOTf-S2 electrolytes at different current densities.

performances.[7] However, although these novel electrolytes have realized reversible Mg anodes with low overpotentials and high CEs and can be prepared with more facile preparation methods through the great efforts of many researchers, these electrolytes still suffer from many other intractable problems, such as the low and unsatisfactory conductivity in the bulk phase, and the poor cathode compatibility due to high de-coordination energy barrier which is caused by the over-strong coordination ability solvents in the solvation structures. For instance, the $MgCl_2$/3-methoxypropylamine (expressed as S2 solvent) electrolyte that was proposed in our previous work has possessed both fast anode interface kinetics and high anode interface stability through the solvent molecule design and anions regulation within the solvation structure.[7a,8] Nevertheless, this well-optimized electrolyte still exhibits poor rate performance and cathode compatibility (**Figure** 1a), which cannot meet the demand of practical batteries. Consequently, the high-performance electrolyte must meet the bulk phase-interface-electrode multi-scale optimization requirement (including ionic conductivity, anode interface stability, and cathode compatibility) and exhibit excellent compatibility with both anode and cathode. Moreover, the potential of electrolyte water resistance still remains worth fully exploring to simplify the processing of electrolyte preparation and promote the application of MMBs.

Herein, we propose a Li/Mg double-salt strategy to achieve the multi-scale optimization of the amine-based electrolyte. The classical lithium triflate (LiOTf) salt is introduced into the representative $MgCl_2$-S2 electrolyte as a multifunctional additive to compensate for the shortcomings of the original electrolyte (Figure 1b). In the bulk phase, the LiOTf salt is sufficiently dissociated to provide sufficient anions and cations in the electrolyte, which significantly improves the electrolyte conductivity (11 times than before) and reduces the overpotential during cycling. At the cathode side, the presence of Li^+ ions with lower surface charge density can accelerate the ions insertion to enhance the cathode compatibility, while Li co-deposition behavior is not able to occur at the anode side owing to their comparatively lower reduction potential compared to Mg^{2+} ions.[9] Moreover, at the anode side, the solvation structures of Mg^{2+} ions are still mainly maintained and the high reduction stability of OTf^- ions avoids anions bond breaking and decomposition behavior in the Mg metal anode/electrolyte interface, ensuring the high anode stability is maintained. Therefore, the Mg//stainless steel (SS) asymmetric cell realizes a high cycling life for 2100 cycles with a remarkable average CE of 99.8% at 1.0 mA cm^{-2}, achieving the goal of improving conductivity while maintaining the anode stability of the original electrolyte. The optimized electrolyte with LiOTf salt enables great improvement in the full cell performances with Mo_6S_8 cathode as well. In addition, attributed to the great water-resistant ability of amine solvent, batteries with $MgCl_2$-LiOTf-S2 electrolyte are preliminarily verified as a proof-of-concept for the air-assembled MMBs. In conclusion, this work proposes an effective additive for the amine-based electrolyte and realizes the good compatibility with the anode and cathode at the same time (Figure 1c).

2. Results and Discussion

The original $MgCl_2$-S2 electrolyte which is proposed in our previous work[8] has achieved rapid charge transfer kinetics and high stability for Mg metal anode because of the optimization of solvent and anion and possesses the advantage of low cost at the same time. However, despite the great compatibility with Mg metal anode and commercial accessibility for the $MgCl_2$-S2 electrolyte, this electrolyte is still difficult to meet the requirements

of high-performance electrolytes for MMBs. The main disadvantages of the $MgCl_2$-S2 electrolyte are as below: low conductivity and poor performance at the cathode side. Thus, the original $MgCl_2$-S2 electrolyte needs the additive salt to improve the corresponding performances and the additive salt needs to meet the following points: i) Additive salt can be completely dissociated within the electrolyte to increase the free anions and cations in order to enhance the conductivity of the electrolyte. ii) Additive salt does not affect the high compatibility of the original electrolyte with Mg metal anode, namely that anion decomposition and cation co-deposition should be avoided. iii) Cation should possess a lower surface charge density compared to the Mg^{2+} ion to facilitate ion insertion process at the cathode side. Based on the analysis above, first, the Mg salt additives are preferentially excluded in the view of cation design because their cations are still Mg^{2+} ions and the cation solvation structures are nearly the same, and thus the performance of the cathode side cannot be improved. The monovalent ions including Li^+ ions and Na^+ ions can be more suitable to meet the demand of cation design. As for the anion design, Cl^- ions are presumed to be difficult to achieve obvious conductivity enhancement due to their poor dissociation in the amine solvent despite its high stability to Mg metal anode. And for the anions including OTf^- ion and $TFSI^-$ ion which can be dissociated more completely in amine solvent, the OTf^- possesses the higher reduction stability compared to $TFSI^-$ ion, which can thus be more likely to maintain the stability of the anode interface as before. The decomposition characteristic of the $TFSI^-$ ion is demonstrated in other literatures[7b,10] and further investigated by experimental verification in this work as well (Figure S1a,b, Supporting Information). Therefore, the LiOTf and NaOTf salts are chosen as two possibly appropriate additive salts to conduct the preparation of optimized electrolytes, namely, $MgCl_2$-LiOTf-S2 electrolyte and $MgCl_2$-NaOTf-S2 electrolyte. However, although the single NaOTf salt can be completely dissolved in the S2 solvent, when it is mixed with the $MgCl_2$ salts in the S2 solvent, the electrolyte becomes muddy. And we conducted an experiment and proved that the mixed dissolution of these two salts in the S2 solvent will lead to the formation of an insoluble NaCl component (Figure S2a–d, Supporting Information). In comparison, the $MgCl_2$-LiOTf-S2 electrolyte exhibits both clarity and transparency (Figure S3, Supporting Information), and thus the LiOTf salt is the only suitable additive for the $MgCl_2$-S2 electrolyte according to the analysis above.

Subsequently, the focus is on examining the most effective concentration of LiOTf additive in the $MgCl_2$-S2 electrolyte, with the test results presented in Figure S4 and Table S1 (Supporting Information). At the beginning, the introduction of LiOTf salt increases the free cations and anions in the electrolyte and thus improves the ionic conductivity. However, with the further increase of the concentration of LiOTf, the viscosity in the electrolyte is significantly increased which instead leads to the decrease of the conductivity. Finally, the 0.5 M LiOTf is considered as the best concentration for the additive of the $MgCl_2$-S2 electrolyte. Other additive salts including LiCl and LiTFSI are studied as well. Due to the presence of Li^+ ions with a low charge density in LiCl salt, the conductivity of the electrolyte can be still further increased even under the unfavorable conditions of increasing the concentration of Cl^- ions in the electrolyte system, indicating the great function of low charge density cations compared to the Mg^{2+} ions in enhancing electrolyte conductivity. Unfortunately, due to the extremely difficult dissociation of Cl^- ions in the S2 solvent, the LiCl salt additive only has a limited effect on the increase of electrolyte conductivity compared to LiTFSI salt or LiOTf salt. As for the LiTFSI salt, although it can be dissociated completely in S2 solvent and significantly increase the electrolyte conductivity, it still has no value for further study and cannot be an effective electrolyte additive due to the occurrence of rapid short-circuit phenomenon in the battery system, which results from the decomposition and passivation effect of the $TFSI^-$ anion. The ionic conductivities of original electrolyte with different additives are summarized in Figure 1d for visual comparison.

The rate performances of the original $MgCl_2$-S2 electrolyte and the $MgCl_2$-S2 electrolyte with LiCl and LiOTf additives are examined in the Mg//Mg symmetric cells (Figure 1e,f; Figure S5a,b, Supporting Information). Regarding to the original $MgCl_2$-S2 electrolyte, it shows an obvious increase in the overpotential as the current density rises and it even cannot run under the current density of 2.0 mA cm^{-2}, which might be caused by the insufficient free ion-pairs to sustain normal electromigration under a high current density. And for the electrolytes with additives, the rate performances are improved obviously. And especially for the $MgCl_2$-LiOTf-S2 electrolyte, it shows the lowest overpotentials among the three electrolytes (only 0.02 V at 0.1 mA cm^{-2} and 0.6 V at 4.0 mA cm^{-2}). The cyclic voltammetry (CV) test shows a similar electrochemical tendency (Figure S6, Supporting Information). These results indicate that the low ionic conductivity and poor rate performance of the original electrolyte can be solved perfectly through the introduction of a suitable additive salt, namely, LiOTf at 0.5 M.

The compatibility between the optimized $MgCl_2$-LiOTf-S2 electrolyte and the Mg metal anode is further studied. As shown in **Figure 2a**, the cycling performance of the $MgCl_2$-LiOTf-S2 electrolyte in the symmetrical Mg coin cells is even more stable than that of the original electrolyte and it exhibits a lower polarization voltage of ≈0.03 V for over 4000 h at 0.1 mA cm^{-2}. The lower overpotential is mainly attributed to the higher ionic conductivity of the $MgCl_2$-LiOTf-S2 electrolyte and thus the ohmic polarization is markedly reduced. The low polarization voltage during cycling can effectively avoid the uncontrollable decomposition of solvent molecules, anions, and other impurity molecules in thermodynamics, which thus benefits to a more stable cycling performance. At a higher current density of 1.0 mA cm^{-2}, the $MgCl_2$-LiOTf-S2 electrolyte shows a similar stable cycling performance with an overpotential of only ≈0.15 V (Figure S7, Supporting Information). The anode reversibility of the optimized electrolyte is also examined (Figure 2b). The asymmetrical Mg//SS cell of the $MgCl_2$-LiOTf-S2 electrolyte shows a remarkably high average CE of 99.8% for over 2100 cycles at the 1.0 mA cm^{-2} with 1.0 mAh cm^{-2}, indicating the decomposition of the OTf^- anion in the electrolyte system is significantly inhibited, and thus the outstanding Mg metal anode interface stability is remained as the original $MgCl_2$-S2 electrolyte. This electrochemical result further demonstrates well-designed LiOTf additive can achieve bulk phase-interface-anode multi-scale optimization, namely, improving the ionic conductivity while preserving the superior stability of the anode and interface. To our current knowledge, in comparison to traditional electrolytes based on the design of solvation structures in other studies,[6a,7,8,11] the $MgCl_2$-LiOTf-S2

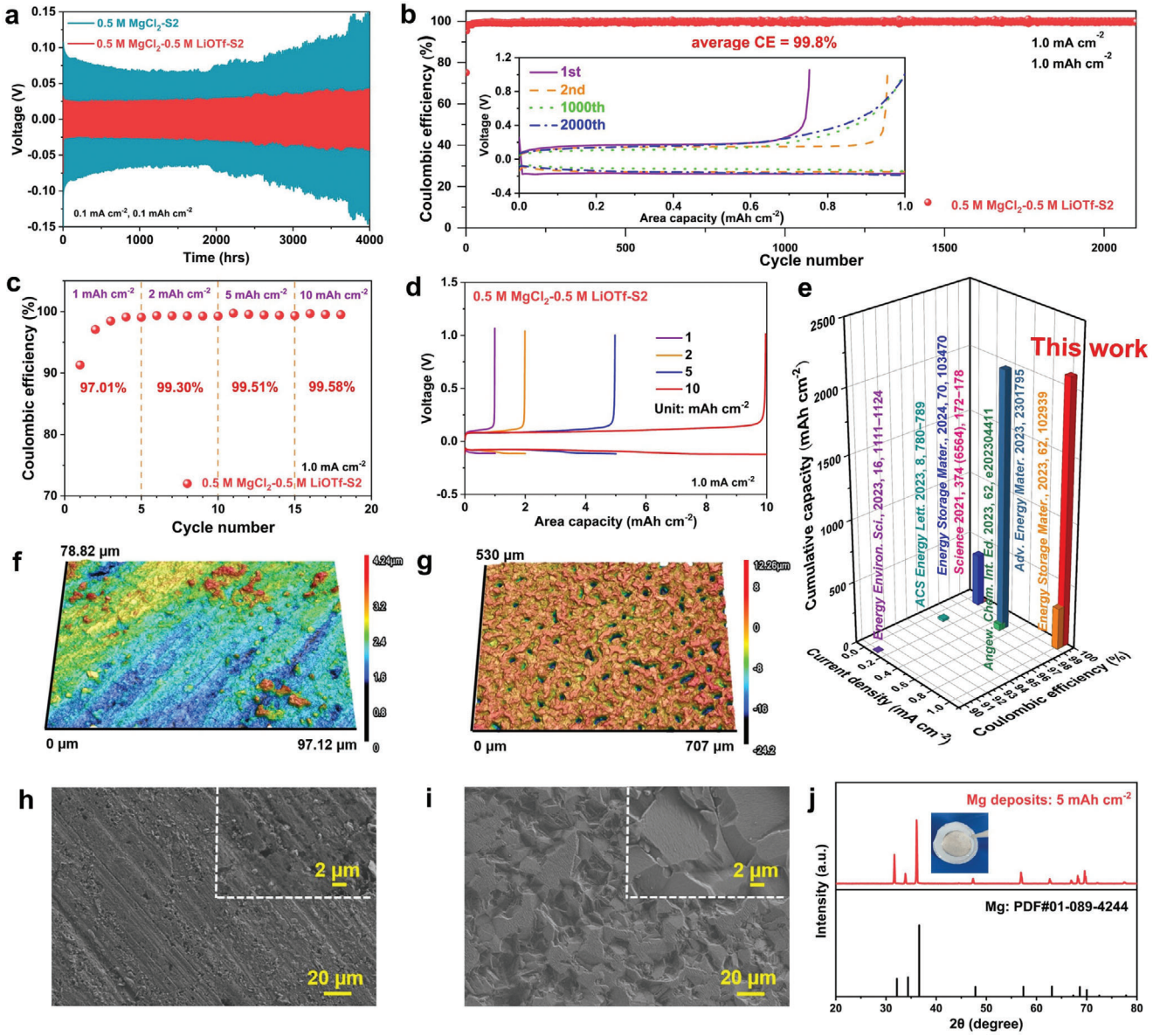

Figure 2. a) The cycling voltage profiles of the $MgCl_2$-S2 electrolyte and the $MgCl_2$-LiOTf-S2 electrolyte in symmetrical Mg coin cells at the current density of 0.1 mA cm^{-2} with 2 h in a single cycle. b) The CE of the $MgCl_2$-LiOTf-S2 electrolyte in the asymmetrical SS coin cell at the current density of 1.0 mA cm^{-2} with 1 h in a single discharge process (Insert is the voltage profiles with different cycle numbers). c) The CEs of different cycling capacities for the $MgCl_2$-LiOTf-S2 electrolyte at 1.0 mA cm^{-2}. d) Voltage profiles of the $MgCl_2$-LiOTf-S2 electrolyte with different discharge capacities at 1.0 mA cm^{-2}. e) Comparisons of current density, average CE and cumulative capacity in this work with recorded information in document literatures. f) Laser microscope image and h) SEM image of the Mg cycling morphology in the $MgCl_2$-LiOTf-S2 electrolyte at the current density of 1.0 mA cm^{-2} with 2 h in a single cycle for 30 cycles. g) Laser microscope image and i) SEM image of the Mg deposition morphology on the Mg metal substrate in the $MgCl_2$-LiOTf-S2 electrolyte at 1.0 mA cm^{-2} with 10.0 mAh cm^{-2}. j) The XRD pattern of Mg deposits for the $MgCl_2$-LiOTf-S2 electrolyte at 1.0 mA cm^{-2} with 5.0 mAh cm^{-2} (Inset is the optical image of the Mg deposits).

electrolyte displays a remarkable electrochemical performance with both the highest average CE and highest cumulative capacity in a relatively high current density (Figure 2e; Table S2, Supporting Information). The Mg//SS asymmetric cell of the $MgCl_2$-LiOTf-S2 electrolyte tested at the current density of 0.1 mA cm^{-2} shows the same high CE as well (Figure S8a,b, Supporting Information). Moreover, the Mg//SS asymmetric cell tested with higher discharge capacities (from 1.0 to 10.0 mAh cm^{-2}) still exhibits good CEs and stable capacity-voltage cycling curves (Figure 2c,d), indicating the anode interface can maintain a high stability as before even under the extreme electrochemical condition. In addition, the linear-sweep voltammetry and water sensitivity of the optimized electrolyte are measured as well (Figures S9 and S10a,b, Supporting Information).

The Mg metal surface morphologies after electrochemical test are observed by laser microscope and scanning electron

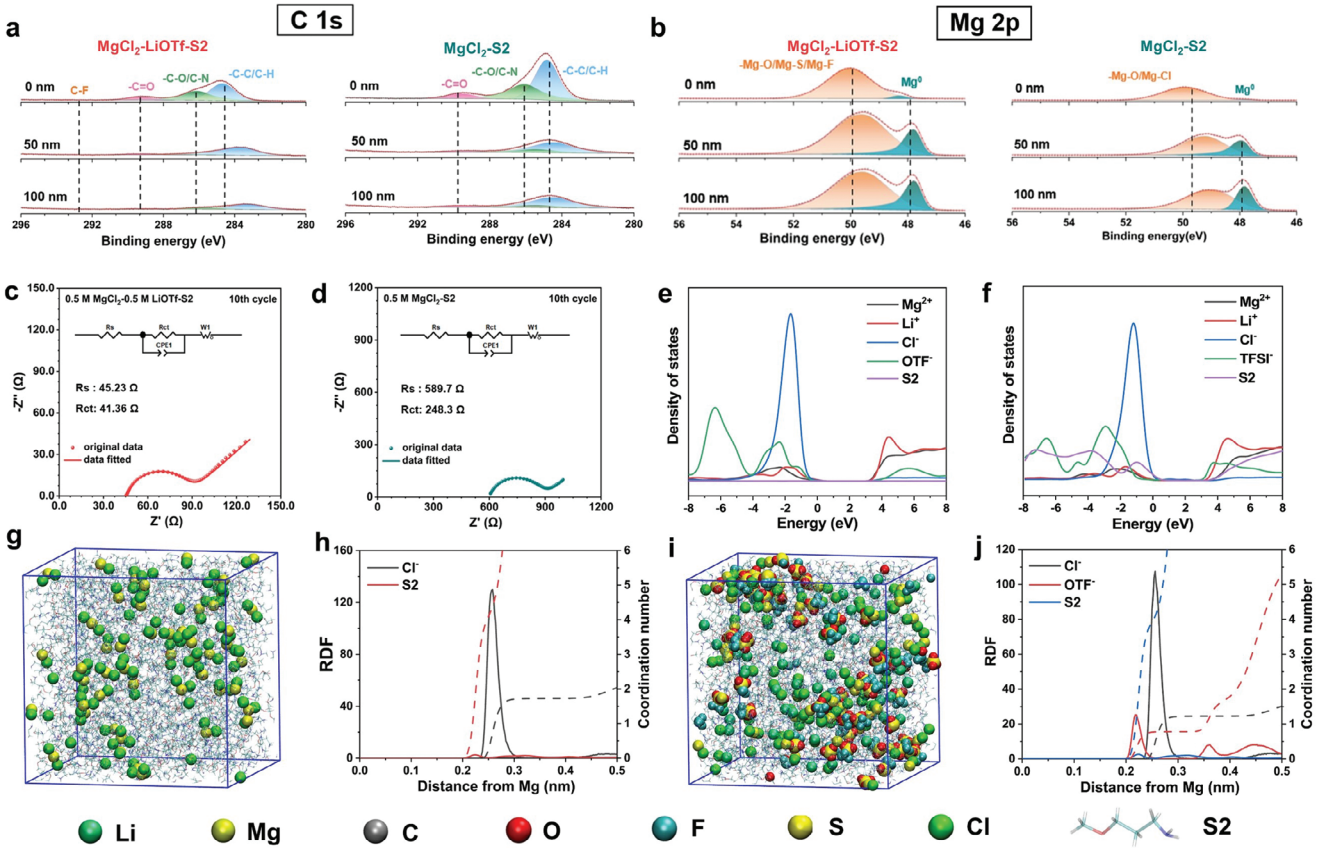

Figure 3. XPS a) C 1s and b) Mg 2p spectra of Mg anodes of the original electrolyte and the optimized electrolyte (symmetrical Mg coin cells are cycled at 0.1 mA cm^{-2} with 1 h for 30 cycles and detected at the end of the stripping state). The Nyquist plots of c) the optimized electrolyte and d) the original electrolyte at the 10th cycle in the Mg//Mg symmetric cells. The PDOS diagrams of e) the $MgCl_2$-LiOTf-S2 electrolyte and f) the $MgCl_2$-LiTFSI-S2 electrolyte. g) Snapshots and h) the RDF of the original electrolyte. i) Snapshots and j) the RDF of the optimized electrolyte.

microscope (SEM). As for the Mg surface morphologies in Figure 2f,h, the Mg metal anodes are obtained in the Mg//Mg symmetric cells for 30 cycles at 1.0 mA cm^{-2} with 1.0 mAh cm^{-2}. Their surface morphologies are smooth nearly without any protrusions or impurity decomposition product can be observed. Besides, even in the low-magnification image of the laser microscope (Figure S11, Supporting Information), no ununiform Mg deposits can be observed, indicating the smooth surface morphologies belong to the whole Mg foils rather than in a small and particular area after cycling. The huge gullies are caused by the pre-cleaning of the Mg metal surface with the sandpaper. As for the Mg surface morphologies in Figure 2g,i, Mg metal anodes are obtained in Mg//SS asymmetric cells with the galvanostatic deposition process at 1.0 mA cm^{-2} with 10.0 mAh cm^{-2}. The electrodeposition Mg metal of high deposition capacity exhibits obvious polyhedral Mg metal deposition morphology without the observation of inhomogeneous and large Mg protrusions, indicating the smooth Mg deposition morphology can still remain even in the strict electrochemical testing condition. Besides, the X-ray diffraction (XRD) measurement is conducted to investigate the components of the Mg deposits (Figure 2j). The characteristic peaks of Mg deposits perfectly match with the reference card of the Mg crystal phase (PDF#01-089-4244) and no obvious characteristic peaks of Li metal and anion decomposition product are detected, indicating the Li co-deposition cannot occur and anion decomposition is restrained as well during the electrodeposition process.[9,12] The optical image of the Mg deposit in Figure 2j also shows a clear gray color with a distinct metallic sheen and a smooth surface morphology, demonstrating the great consistency between the macroscopic visual observation and the microscopic detection. The cycling performance of the symmetrical Mg//Mg cell of the $MgCl_2$-LiOTf-S2 electrolyte cycling with the polypropylene (PP, celagrd) separator rather than the glass fiber (GF, Whatman) separator is also tested (Figure S12a, Supporting Information). The thickness of the PP separator (≈15–20 µm) is far thinner than that of the GF separator (≈400–500 µm), which is more likely to cause the internal short-circuit for MMBs. The test result shows that the $MgCl_2$-LiOTf-S2 electrolyte with PP separator can still run stably for over 400 h with an overpotential of ≈0.04 V, further demonstrating the uniform Mg deposition of the optimized electrolyte. But as for the classical $Mg(TFSI)_2$-DME electrolyte, the Mg//Mg coin cell becomes short-circuit sharply within the first 3 cycles (Figure S12b, Supporting Information).

The differences in surface components for Mg anode are measured by X-ray photoelectron spectroscopy (XPS) before and after the addition of LiOTf salt in the original $MgCl_2$-S2 electrolyte (**Figure 3**a,b).[6a,7b,8] According the common sense, introducing the LiOTf salt containing the OTf^- anions that possess the

decomposition possibility to a certain degree into a highly stable electrolyte, will inevitably increase the decomposition products of Mg anodes during the battery cycling. However, the XPS measurement results indicate that the electrolyte decomposition species within the $MgCl_2$-LiOTf-S2 electrolyte do not increase but even decrease compared to those of the original $MgCl_2$-S2 electrolyte. In addition to the intrinsic high stability of the OTf^- anion (Figure 3e,f, as described later), the reason can also be attributed to the fact that after the addition of the LiOTf salt, the decomposition of each component within the electrolyte, including solvents, anions, and impurity molecules, is avoided because of the significant increase in the electrolyte conductivity that reduces the overpotential during cycling, which is in consistent with the cycling performances in the Mg//Mg symmetric cells (Figure 2a). These results show that the high anode stability of the original $MgCl_2$-S2 electrolyte is well-retained and even enhanced. These are further verified by energy-dispersive spectroscopy (EDS) mapping measurement results (Figures S13–S15, Supporting Information). The anode stability is also investigated by electrochemical impedance spectroscopy (EIS). As shown in Figure 3c,d, the optimized electrolyte displays a lower ohmic impedance (Rs, 45.23 Ω) and a lower interface charge transfer impedance (Rct, 41.36) compared to those of the $MgCl_2$-S2 electrolyte (589.7 Ω for Rs and 248.3 Ω for Rct), indicating its faster interface charge transfer kinetics due to the more fresh Mg anode and its obviously improved conductivity after the addition of the LiOTf salt. Besides, the $MgCl_2$-LiOTf-S2 electrolyte shows a stable interface impedance during long cycling as well (Figure S16, Supporting Information). In addition, we carry out an experiment to illustrate the good electrochemical performances of the $MgCl_2$-LiOTf-S2 electrolyte are not dominated by the formation of Mg^{2+}-conductive interfacial layer. As shown in Figure S17 (Supporting Information), the Mg anodes are disassembled from the symmetrical Mg coin cells cycled in the $MgCl_2$-LiOTf-S2 electrolyte after 30 cycles, and these cycled Mg foils are reassembled into two new symmetrical Mg coin cells with the 0.5 M $Mg(TFSI)_2$-DME electrolyte and 0.5 M $MgCl_2$-0.5 M LiOTf-S2 electrolyte, respectively. As for the new symmetric cell with the 0.5 M $Mg(TFSI)_2$-DME electrolyte, its electrochemical performance is not improved, and even for the first few cycles the overpotential is still kept at ≈2 V. While for the symmetrical Mg coin cell with the 0.5 M $MgCl_2$-0.5 M LiOTf-S2 electrolyte, its electrochemical performance remains as before.

To explore the reason why the OTf- anion is difficult to be reduced and further decomposed to form by-products in the electrolyte system compared to the $TFSI^-$ anion, the projected density of state (PDOS) analysis is performed by the density functional theory (DFT) calculations (Figure 3e,f). In the optimized electrolyte, the foremost valence band is still allocated to divalent Mg ions rather than OTf^- or Li^+ ions after the addition of the LiOTf salts, which is the same tendency as the original $MgCl_2$-S2 electrolyte. This result indicates that the Mg^{2+} ions are more likely to gain electrons and further reduced to form the metallic Mg atoms in thermodynamics during the interface electron transfer process, which avoids the occurrence of the decomposition of OTf^- anions and the co-deposition of Li metal. Thus, this DFT data demonstrates the LiOTf additive salt does not affect the high compatibility of the original $MgCl_2$-S2 electrolyte with Mg anodes. While as for the original electrolyte with the LiTFSI additive, the foremost valence band is not allocated to divalent Mg ions but $TFSI^-$ anions, manifesting the decomposition of $TFSI^-$ ions can happen thermodynamically. The uncontrollable anion decomposition reaction will lead to the deterioration of the Mg anode and limit the battery life eventually.

The solvated structure of the optimized electrolyte is further inspected and compared with that of the original electrolyte by the molecular dynamic simulation (Figure 3g–j). In the $MgCl_2$-S2 electrolyte, the coordination numbers of the Cl^- ion and S2 with the Mg^{2+} ions are 4.0 and 1.92, respectively, indicating that Mg^{2+} ions coordinated with two solvent molecules and two Cl^- ions are the majority solvation structures in the electrolyte system. Besides, according to our previous work,[8] nearly all the Mg^{2+} ions are coordinated with one or two Cl^- ions, thus leading to a severe anion-cation association situation and showing an extremely low ionic conductivity of the electrolyte. While in the optimized electrolyte, after the introduction of LiOTf salt, part of the OTf^- can participate in the first solvation sheath of Mg^{2+} ion and replace the coordination of the S2 solvent and especially the Cl^- ion. This is further confirmed by the nuclear magnetic resonance (NMR) measurement results (Figure S18, Supporting Information). The weakened Mg^{2+}-Cl^- association situation in the optimized electrolyte can promote the electromigration of the Mg^{2+} ions in the bulk phase. Moreover, the dissociation situation of LiOTf salt in the S2 solvent is studied as well (Figure S19a–c, Supporting Information). In the LiOTf-S2 electrolyte, Li^+ ions are nearly all coordinated with S2 solvents, indicating the LiOTf salt is sufficiently dissociated in the S2 solvent. And in the original electrolyte with LiOTf additive, the solvation structures of Li^+ ions are substantially maintained. Li^+ ions are still mainly coordinated with S2 solvents rather than the OTf^- anions or Cl^- anions, demonstrating that the LiOTf additive can provide large free anions and cations in the electrolyte and thus effectively enhance the electrolyte conductivity and improve the rate performances of the batteries.

The performances of full cells with the classical intercalation-type Mo_6S_8 cathode are investigated. As shown in **Figure 4a,b**, the full cell with the $MgCl_2$-LiOTf-S2 electrolyte exhibits a good rate performance and can deliver a high discharge capacity of ≈77 mAh g^{-1} even at the rate of 5 C (1 C = 128.8 mA g^{-1}). While for the original $MgCl_2$-S2 electrolyte, due to the low electrolyte conductivity, high intercalation energy barrier of divalent Mg^{2+} ions, and the solvation structure with severe anion-cation association situation, the full cell of the $MgCl_2$-S2 electrolyte shows an obviously low rate performance and can only deliver a discharge capacity of 30 mAh h^{-1} at the rate of 1 C and even 6 mAh g^{-1} at the rate of 2 C (Figure S20a,b, Supporting Information). The long-cycling performances are further studied as well. The full cell with the $MgCl_2$-LiOTf-S2 electrolyte can operate stably at the rate of 5 C for 1000 cycles with a high CE of nearly 100% and exhibits a good capacity retention of ≈62.4% after cycling (Figure 4c). In contrast, the full cell with the $MgCl_2$-S2 electrolyte runs unstably and only delivers a low capacity of ≈10 mAh g^{-1} after 200 cycles even just at the rate of 1 C, which is worse than that of the optimized electrolyte (Figure S20c,d, Supporting Information). The difference in the interface impedance before and after the addition of the LiOTf salt into the original $MgCl_2$-S2 electrolyte is measured (Figure 4d). The activated carbon is chosen as the anode rather the Mg foil, which aims at avoiding the effect of the anode side (Figure S21a,b, Supporting Information). Compared

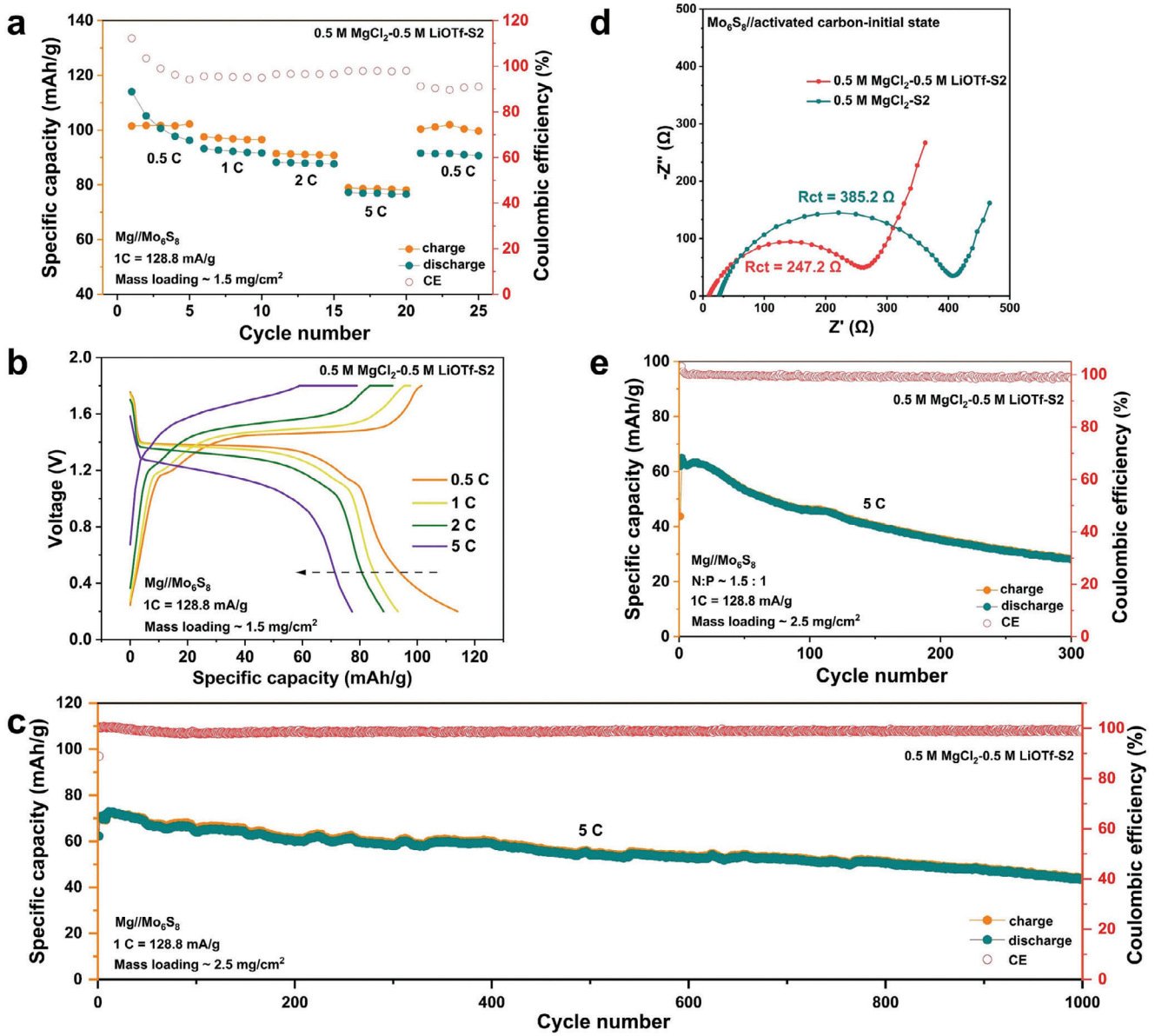

Figure 4. a) Rate performance of the optimized electrolyte in the Mg//Mo6S8 full cell from 0.5 C to 5 C (0.5 C, 1.0 C, 2.0 C, 5.0 C and 0.5 C; 1 C = 128.8 mA g^{-1}). b) Voltage profiles of the optimized electrolyte in the Mg//Mo6S8 full cells at the rates of 0.5 C, 1 C, 2 C, and 5 C. c) The long cycling performance of the Mg//Mo6S8 full cell with the optimized electrolyte at the rate of 5 C. d) Nyquist plots of the original electrolyte and optimized electrolyte with Mo6S8 cathode in the initial state. e) The long cycling performance of the limited Mg//Mo_6S_8 full cell with the optimized electrolyte at the rate of 5 C (N:P = 1.5:1).

to the original electrolyte, the $MgCl_2$-LiOTf-S2 electrolyte shows an obviously lower Rct (247.2 Ω vs 385.2 Ω), indicating the Li^+ ions with low surface charge density can reduce the energy barrier and accelerate the ion insertion process at the cathode side, and thus effectively promoting compatibility between the cathode and electrolyte.[13] The contribution of Li intercalation is also investigated by the inductively coupled plasma-optical emission spectrometry (ICP-OES) measurement (Table S3, Supporting Information). Besides, most of the tests conducted on MMBs are based on the far excess Mg metal anode. This is not only inconsistent with the metal battery concept for which it was proposed at the beginning but also fails to demonstrate the advantages of Mg metal in terms of high volumetric energy density. Thus, the full cell with the limited Mg metal anode is tested as well. The limited Mg metal anode is prepared by electrodepositing a certain amount of Mg metal according to the mass loading of the cathode into the SS current collector. As shown in Figure 4e, the capacity ratio of the negative electrode and positive electrode (N:P ratio) is controlled at 1.5:1. Even in such a strict electrochemical testing condition, the full cell with the $MgCl_2$-LiOTf-S2 electrolyte can still run for over 300 cycles at the rate of 5 C with a CE of ≈100%, demonstrating the optimized $MgCl_2$-LiOTf-S2

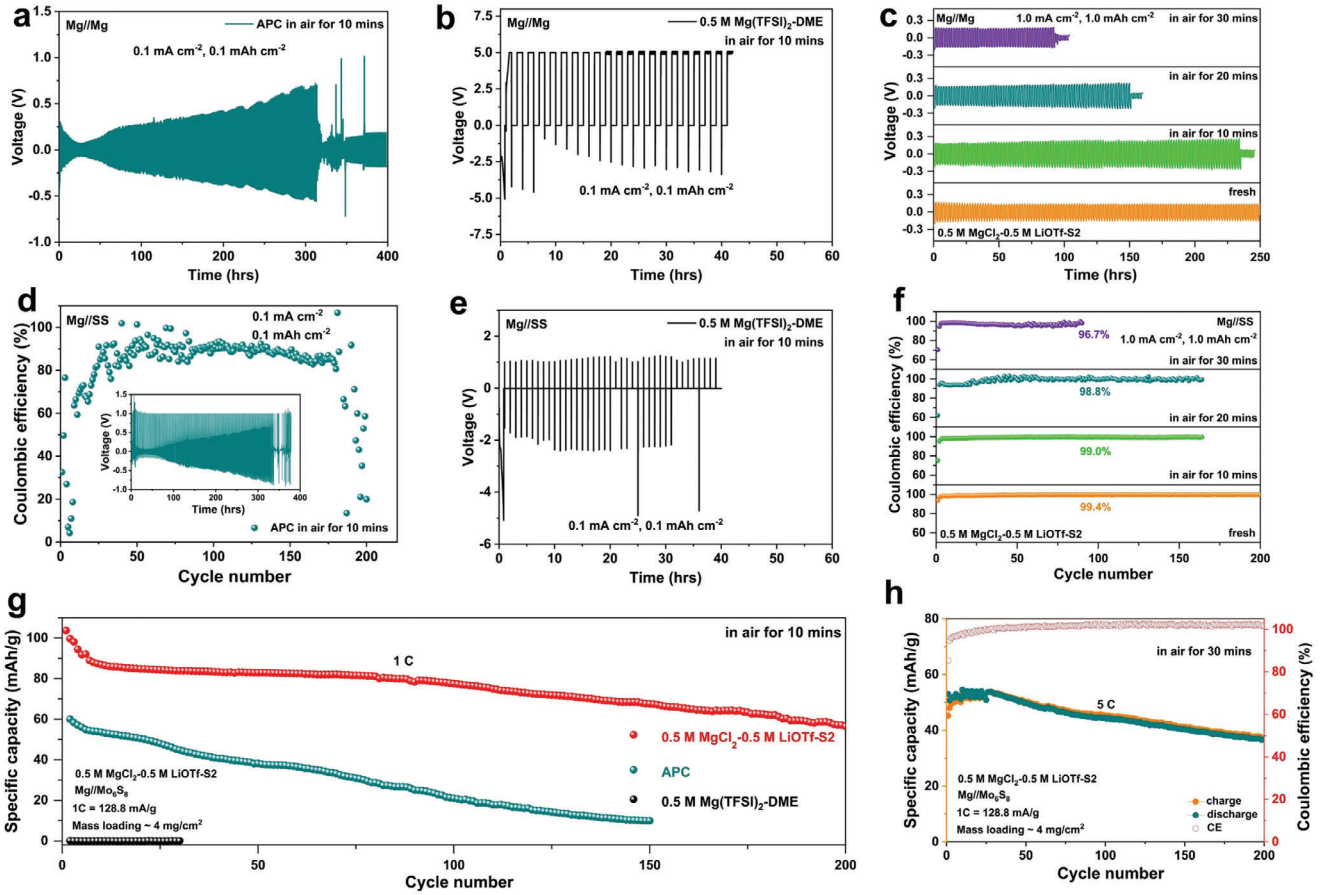

Figure 5. The cycling performances in symmetrical Mg coin cells for a) APC, b) 0.5 M $Mg(TFSI)_2$-DME, and c) 0.5 M $MgCl_2$-0.5 M LiOTf-S2 electrolytes after exposure to air. The CE tests in Mg//SS asymmetric cells d) APC, e) 0.5 M $Mg(TFSI)_2$-DME and f) 0.5 M $MgCl_2$-0.5 M LiOTf-S2 electrolytes after exposure to air. g) Full-cell performances of Mg//Mo_6S_8 for three types of electrolytes at the rate of 1 C after exposure to air. h) Full-cell performance of the 0.5 M $MgCl_2$–0.5 M LiOTf-S2 electrolyte in the Mg//Mo_6S_8 at the rate of 5 C after exposure to air for 30 min.

electrolyte can achieve the extremely high utilization of the Mg metal anode and realize the good compatibility with both anode and cathode as expected.

The electrolyte which is the crucial component of the battery system is very sensitive to the air environment because the water can dissolve into the electrolyte which leads to the passivation of the Mg metal anode and effective components of the electrolyte could react with air (such as oxygen, water, and carbon dioxide) as well, leading to the deterioration of the electrolyte eventually. And thus, the assemblies of MMBs are all conducted in the glove boxes to avoid the adverse influence of water and oxygen on the battery system especially on the electrolyte. However, the electrolytes with amine solvents possess a great water-resistant ability compared to traditional ether-based electrolytes, which has been examined and illustrated in detail in our previous work.[7a] Besides, the solutes of the amine-based electrolytes are all convention simple Mg salts which are difficult to react with the components in the air directly. Therefore, the batteries with amine-based electrolytes possess the great potential and possibility to be assembled in the air environment. Herein, as an attempt, we choose the optimized $MgCl_2$-LiOTf-S2 electrolyte and two other electrolytes, namely, all phenyl complex (APC) electrolyte[4b] and $Mg(TFSI)_2$-DME electrolyte,[14] to verify the possibility of the assembly of MMBs in the air environment.

First, the normal electrochemical performances of the APC electrolyte and the $Mg(TFSI)_2$-DME electrolyte are tested and the results are in good agreement with the data reported in the literatures,[6a,15] indicating the successful synthesis of these two electrolytes (Figure S22a–d, Supporting Information). Then, these two electrolytes and the $MgCl_2$-LiOTf-S2 electrolyte are all transferred into the air environment and are left exposed to air directly for some time. Subsequently, we assemble the Mg//Mg batteries with these electrolytes to test the changes in electrochemical performances (Mg foils are still polished and fresh). As shown in **Figure 5**a–f, the performances of APC electrolyte and $Mg(TFSI)_2$-DME electrolyte deteriorate significantly, including the increase of the overpotential and the decrease of the CE, which is consistent with the traditional recognition that the electrolyte has a high air sensitivity. While for the $MgCl_2$-LiOTf-S2 electrolyte, although its electrochemical performance also decreases slightly (the degree of decrease increased with the placing times), it can still support a highly reversible Mg deposition/stripping process even at the placing time of 30 min. This result demonstrates that the $MgCl_2$-LiOTf-S2 electrolyte possesses a good air-stable performance and thus it can support further

verification about the possibility of the assembly of MMBs in the air environment. The air stability of the Mo_6S_8 cathode and the Mg metal anode is also examined (Figures S23, S24a,b, and S25a,b, Supporting Information). The measurement results indicate that the cathode materials and the anode materials have the high air stability, and the electrochemical performances are hardly influenced even the cathode and anode are placed in the air environment for 7 days.

The MMBs assembled in the air environment are consist of the Mo_6S_8 cathodes and the Mg metal anodes which are both placed in the air for 7 days, and the electrolytes are left exposed to air directly for 10 min. As shown in Figure 5g, only the battery with the $MgCl_2$-LiOTf-S2 electrolyte can maintain normal circulation for 200 cycles. Even for the $MgCl_2$-LiOTf-S2 electrolyte left exposed to air directly for 30 min (Figure 5h), the according battery can still run at a rate of 5 C for 200 cycles. In conclusion, the batteries with $MgCl_2$-LiOTf-S2 electrolyte are preliminarily verified as a proof-of-concept for the air-assembled MMBs, which possess the good potential of simplifying the production process and promoting the practical application of MMBs.

3. Conclusion

In summary, we propose a Li/Mg double-salt electrolyte based on the amine solvent ($MgCl_2$-LiOTf-S2 electrolyte) to achieve the bulk phase-interface-electrode multi-scale optimization, including ionic conductivity, anode interface stability and cathode compatibility. The classical LiOTf salt is introduced into the $MgCl_2$-S2 electrolyte as a multifunctional additive to compensate for the shortcomings of the original electrolyte. The final selection of the LiOTf salt is based on the comprehensive anion-cation design analysis and experimental verification. The LiOTf salt can be sufficiently dissociated in the electrolyte to provide sufficient anions and cations in the bulk phase, significantly improving the ionic conductivity of the electrolyte and observably reducing the overpotential during cycling. And at the cathode side, the presence of Li^+ ions with lower surface charge density can accelerate the ions insertion to enhance the cathode compatibility, while Li codeposition behavior is not able to occur at the anode side at the same time owing to their comparatively lower reduction potential compared to Mg^{2+} ions. Moreover, the high reduction stability of OTf^- ions can avoid anions bond breaking behaviors and the decomposition occurrence in the Mg metal anode/electrolyte interface, ensuring the high anode stability is maintained. Benefitting from these, the Mg//SS asymmetric cell finally realizes the ultrahigh cycling life for over 2100 cycles with a remarkable average CE of ≈99.8% at 1.0 mA cm^{-2} and the Mg//Mo_6S_8 full cell can also run stably even at the rate of 5 C for 1000 cycles with a good capacity retention of ≈62.4%. In addition, the batteries with the optimized electrolyte are verified as a proof-of-concept for the air-assembled MMBs. The battery with the $MgCl_2$-LiOTf-S2 electrolyte which is left exposed to air directly for 30 min can still run at a rate of 5 C for 200 cycles with a CE of nearly 100%. This work emphasizes the important function of the multifunctional additive in enhancing the compatibility between anodes and cathodes with amine-based electrolytes in MMBs.

Supporting Information

Supporting Information is available from the Wiley Online Library or from the author.

Acknowledgements

F.W. and H.H. contributed equally to this work. The authors gratefully acknowledge the National Key Research and Development Program of China (No. 2021YFB2400300), the Natural Science Foundation of China (Nos. 21875198, 22005257, and 22021001), the Natural Science Foundation of Fujian Province of China (No. 2020J05009) and Natural Science Foundation Project of Xiamen city (No. 3502Z202471026) for financial support.

Conflict of Interest

The authors declare no conflict of interest.

Data Availability Statement

Research data are not shared.

Keywords

compatibility with anode and cathode, conductivity, Li/Mg double-salt strategy, Mg metal batteries, multi-scale optimization

Received: August 5, 2024
Revised: September 3, 2024
Published online: September 27, 2024

[1] a) P. Bonnick, J. Muldoon, *Adv. Funct. Mater.* **2020**, *30*, 1910510; b) Z. Liang, C. Ban, *Angew. Chem., Int. Ed.* **2021**, *60*, 11036; c) J. Muldoon, C. B. Bucur, T. Gregory, *Angew. Chem., Int. Ed.* **2017**, *56*, 12064; d) J. Zhang, Z. Chang, Z. Zhang, A. Du, S. Dong, Z. Li, G. Li, G. Cui, *ACS Nano* **2021**, *15*, 15594.

[2] a) J. Muldoon, C. B. Bucur, T. Gregory, *Chem. Rev.* **2014**, *114*, 11683; b) H. D. Yoo, I. Shterenberg, Y. Gofer, G. Gershinsky, N. Pour, D. Aurbach, *Energy Environ. Sci.* **2013**, *6*, 2265.

[3] a) M. Rashad, M. Asif, Y. X. Wang, Z. He, I. Ahmed, *Energy Storage Mater.* **2020**, *25*, 342; b) R. Mohtadi, O. Tutusaus, T. S. Arthur, Z. Zhao-Karger, M. Fichtner, *Joule* **2021**, *5*, 581; c) C. L. You, X. W. Wu, X. H. Yuan, Y. H. Chen, L. L. Liu, Y. S. Zhu, L. J. Fu, Y. P. Wu, Y. G. Guo, T. van Ree, *J. Mater. Chem. A* **2020**, *8*, 25601; d) P. Saha, M. K. Datta, O. I. Velikokhatnyi, A. Manivannan, D. Alman, P. N. Kumta, *Prog. Mater. Sci.* **2014**, *66*, 1.

[4] a) D. Aurbach, Z. Lu, A. Schechter, Y. Gofer, H. Gizbar, R. Turgeman, Y. Cohen, M. Moshkovich, E. Levi, *Nature* **2000**, *407*, 724; b) O. Mizrahi, N. Amir, E. Pollak, O. Chusid, V. Marks, H. Gottlieb, L. Larush, E. Zinigrad, D. Aurbach, *J. Electrochem. Soc.* **2008**, *155*, A103.

[5] a) R. Mohtadi, M. Matsui, T. S. Arthur, S. J. Hwang, *Angew. Chem., Int. Ed.* **2012**, *51*, 9780; b) T. J. Carter, R. Mohtadi, T. S. Arthur, F. Mizuno, R. Zhang, S. Shirai, J. W. Kampf, *Angew. Chem., Int. Ed.* **2014**, *53*, 3173; c) O. Tutusaus, R. Mohtadi, T. S. Arthur, F. Mizuno, E. G. Nelson, Y. V. Sevryugina, *Angew. Chem., Int. Ed.* **2015**, *54*, 7900.

[6] a) S. Hou, X. Ji, K. Gaskell, P.-F. Wang, L. Wang, J. Xu, R. Sun, O. Borodin, C. Wang, *Science* **2021**, *374*, 172; b) Z. Li, D. T. Nguyen, J. D. Bazak, K. S. Han, Y. Chen, V. Prabhakaran, T. T. Le, Z. Z. Cheng, M. Y. Song, V. G. Pol, K. T. Mueller, V. Murugesan, *Adv. Energy Mater.* **2024**, *14*, 2301544; c) Z. Z. Yang, L. H. Gao, N. J. Leon, C. Liao, B. J. Ingram, L. Trahey, *ACS Appl. Energ. Mater.* **2024**, *7*, 1666.

[7] a) F. Wang, H. M. Hua, D. Z. Wu, J. L. Li, Y. Q. Xu, X. Z. Nie, Y. C. Zhuang, J. Zeng, J. B. Zhao, *ACS Energy Lett.* **2023**, *8*, 780; b) D. Zhang, Y. R. Wang, Y. Yang, Y. Zhang, Y. Z. Zhao, M. Pan, Y. K. Sun, S. P. Chen, X. S. Liu, J. L. Wang, Y. NuLi, *Adv. Energy Mater.* **2023**, *13*, 2301795.

[8] H. M. Hua, F. Wang, F. Wang, J. Y. Wu, Y. Q. Xu, Y. C. Zhuang, J. Zeng, J. B. Zhao, *Energy Storage Mater.* **2024**, *70*, 103470.

[9] H. Y. Fan, X. X. Zhang, Y. X. Zhao, J. H. Xiao, H. Yuan, G. Wang, Y. T. Lin, J. F. Zhang, L. D. Pan, T. Pan, Y. Liu, Y. G. Zhang, *Energy Environ. Mater.* **2023**, *6*, e12327.

[10] D. Zhang, S. Z. Duan, X. S. Liu, Y. Yang, Y. Zhang, W. Ren, S. X. Zhang, M. X. Cheng, W. J. Yang, J. L. Wang, Y. NuLi, *Nano Energy* **2023**, *109*, 108257.

[11] a) J. L. Zhang, J. Liu, M. Wang, Z. H. Zhang, Z. F. Zhou, X. Chen, A. B. Du, S. M. Dong, Z. J. Li, G. C. Li, G. L. Cui, *Energy Environ. Sci.* **2023**, *16*, 1111; b) S. Y. Wang, K. W. Wang, Y. C. Zhang, Y. L. Jie, X. P. Li, Y. X. Pan, X. W. Gao, Q. S. Nian, R. G. Cao, Q. Li, S. H. Jiao, D. S. Xu, *Angew. Chem., Int. Ed.* **2023**, *62*, 202304411; c) Y. Y. Du, Y. M. Chen, S. S. Tan, J. L. Chen, X. T. Huang, L. M. Cui, J. C. Long, Z. T. Wang, X. H. Yao, B. Shang, G. S. Huang, X. Y. Zhou, L. J. Li, J. F. Wang, F. S. Pan, *Energy Storage Mater.* **2023**, *62*, 102939.

[12] J. H. Xiao, X. X. Zhang, H. Y. Fan, Q. Y. Lin, L. D. Pan, H. W. Liu, Y. Su, X. Z. Li, Y. P. Su, S. Y. Ren, Y. T. Lin, Y. G. Zhang, *Adv. Energy Mater.* **2022**, *12*, 2202602.

[13] a) D. Wu, F. Wang, H. Yang, Y. Xu, Y. Zhuang, J. Zeng, Y. Yang, J. Zhao, *Energy Storage Mater.* **2022**, *52*, 94; b) K. Tang, A. B. Du, S. M. Dong, Z. L. Cui, X. Liu, C. L. Lu, J. W. Zhao, X. H. Zhou, G. L. Cui, *Adv. Mater.* **2020**, *32*, 1904987.

[14] S. Y. Ha, Y. W. Lee, S. W. Woo, B. Koo, J. S. Kim, J. Cho, K. T. Lee, N. S. Choi, *ACS Appl. Mater. Interfaces* **2014**, *6*, 4063.

[15] a) Z. Song, Z. Zhang, A. Du, S. Dong, G. Li, G. Cui, *Adv. Mater.* **2021**, *33*, 2100224; b) F. Wang, D. Z. Wu, Y. C. Zhuang, J. L. Li, X. Z. Nie, J. Zeng, J. B. Zhao, *ACS Appl. Mater. Interfaces* **2022**, *14*, 31148.